A cotranscriptional model for 3′-end processing of the *Saccharomyces cerevisiae* pre-ribosomal RNA precursor

ANTHONY K. HENRAS,[1] EDOUARD BERTRAND,[2] and GUILLAUME CHANFREAU[1]

[1]Department of Chemistry and Biochemistry and the Molecular Biology Institute, University of California, Los Angeles, Los Angeles, California 90095-1569, USA

[2]Institut de Génétique Moléculaire de Montpellier (IGMM), Unité Mixte de Recherche (UMR) du Centre National de la Recerche Scientifique (CNRS), IFR 24, 34293 Montpellier Cedex 5, France

ABSTRACT

Cleavage of the *Saccharomyces cerevisiae* primary ribosomal RNA (rRNA) transcript in the 3′ external transcribed spacer (ETS) by Rnt1p generates the 35S pre-rRNA, the earliest detectable species in the pre-rRNA processing pathway. In this study we show that Rnt1p is concentrated in a subnucleolar dot-shaped territory distinct from the nucleolar body. The 35S pre-rRNA is localized at the periphery of the Rnt1p dot, in a pattern that suggests a diffusion of the 35S pre-rRNA from the site of Rnt1p processing. When plasmid-borne versions of the rDNA are used to express rRNAs, the Rnt1p territory reorganizes around these plasmids, suggesting a close association between Rnt1p and the plasmid-borne rDNA units. Rnt1p was found associated with the endogenous rDNA by chromatin immunoprecipitation. Deletion of functionally important Rnt1p domains result in a loss of the dot-shaped territory, showing that this subnucleolar territory corresponds to a functional site of processing. These results show that a large fraction of Rnt1p is localized at the site of transcription of the rDNA, suggesting that the cleavage of the primary pre-rRNA transcript to generate the 35S pre-rRNA is a cotranscriptional event.

Keywords: nucleolus; RNase III; endonuclease; nuclear import

INTRODUCTION

The RNase III family of ribonucleases forms an evolutionary conserved set of enzymes whose members have been identified from bacteria to human (Nicholson 1999; Lamontagne et al. 2001). These enzymes are characterized by their ability to bind directly to double-stranded RNAs (dsRNAs) through a dsRNA-binding domain (dsRBD) and introduce staggered endonucleolytic cleavages within the bound substrates through a typical nuclease domain containing the RNase III signature motif. The genome of the yeast *Saccharomyces cerevisiae* encodes a unique protein containing the RNase III signature motif, Rnt1p (Abou Elela et al. 1996). Although Rnt1p is not essential for yeast viability, the deletion of the *RNT1* gene induces a severe growth defect (Abou Elela and Ares 1998; Chanfreau et al. 1998b). Rnt1p is required for the processing of many cellular noncoding RNAs such as rRNAs (Abou Elela et al. 1996; Kufel et al. 1999), four of the five snRNAs (Chanfreau et al. 1997; Abou Elela and Ares 1998; Allmang et al. 1999; Seipelt et al. 1999), and many small nucleolar RNAs (snoRNAs; Chanfreau et al. 1998a,b; Qu et al. 1999; Lee et al. 2003). All these RNAs are initially synthesized as precursor transcripts that contain additional sequences besides the mature RNAs. Rnt1p initiates the maturation of these precursors by cleaving stem-loop structures in the sequences to be removed. Cleavage in these regions generate entry sites for exoribonucleases that further process these cleaved intermediates into the mature molecules (Allmang et al. 1999; Qu et al. 1999; Lee et al. 2003). The function of Rnt1p is not solely devoted to the maturation of noncoding RNAs. Rnt1p cleavage sites have been identified in the introns of pre-messenger RNAs (pre-mRNAs) encoding ribosomal proteins, and the enzyme has been shown to take part in the turnover of unspliced pre-mRNAs and lariat introns of these transcripts (Danin-Kreiselman et al. 2003).

Rnt1p RNA substrates include a variety of transcripts that are synthesized by different transcription machineries (RNA polymerase I or II), presumably in different nuclear territories. Some of them are processed into mature RNAs that function in the nucleus and do not exit this compartment at any stage of their biogenesis. Thus, Rnt1p must be present

Reprint requests to: Guillaume Chanfreau, Department of Chemistry and Biochemistry and the Molecular Biology Institute, University of California Los Angeles, Box 951569, Los Angeles, CA 90095-1569, USA; e-mail: guillom@chem.ucla.edu; fax: (310) 206-4038.

Article published online ahead of print. Article and publication date are at http://www.rnajournal.org/cgi/doi/10.1261/rna.7750804.

inside the nucleus to take part in the maturation of these specific transcripts. However, whether the enzyme is exclusively nuclear, nucleolar, or also functions in the cytoplasm is unknown so far. Rnt1p is expected to be present in the nucleolus to take part in the maturation of the pre-rRNA but also in the nucleoplasm to process the precursors of snRNAs and snoRNAs as well as to take part in the turnover of intron-containing mRNAs. Although the known functions of Rnt1p provide clues concerning the localization of the enzyme, the detail of Rnt1p localization remain unclear.

The precise timing of the cleavage events catalyzed by the enzyme during the expression of the target RNAs is not fully understood. Rnt1p substrates can be cleaved in vitro in the absence of transcription (Chanfreau et al. 1997, 1998a,b, 2000), but these observations do not rule out cotranscriptional processing in vivo. In particular, the pre-rRNA primary transcript, which is the most abundant Rnt1p substrate in the cell, is hardly detectable in vivo. In wild-type yeast cells, the earliest ribosomal RNA processing intermediate detectable by Northern blot corresponds to the 35S pre-rRNA, which results from the cleavage of the initial primary rRNA transcript by Rnt1p. The fact that the initial primary transcript itself is not detectable has led to the hypothesis that the cleavage step carried out by Rnt1p is cotranscriptional (Allmang and Tollervey 1998). Alternatively, it is possible that cleavage occurs rapidly after transcription termination, resulting in a lack of detection of the primary transcript using standard assays. In support of this hypothesis, transcripts corresponding to the bona fide primary pre-ribosomal RNAs and including the Rnt1p cleavage site can be detected using approaches that are more sensitive than Northern blot (Reeder et al. 1999). Further support for a cotranscriptional model of 3′-end processing of the 3′ ETS was provided by a recent study showing that transcription termination is inhibited in a yeast strain lacking Rnt1p (Prescott et al. 2004).

To answer the question of the localization of Rnt1p, and to try to elucidate the timing of the pre-rRNA processing event catalyzed by Rnt1p, we have studied its subcellular localization. Rnt1p can be detected only within the nuclear compartment of the cells and not in the cytoplasm. In the nucleus, Rnt1p is homogenously distributed throughout the nucleoplasmic region and appears more concentrated within the nucleolus. Rnt1p concentrates within a discrete subnucleolar domain that is likely to correspond to the territory of the nucleolus where Rnt1p participates in the maturation of the pre-rRNA. The 32 carboxy-terminal amino acids of Rnt1p contain a canonical nuclear localization signal that governs the import of the protein into the nucleus. Deletion of Rnt1p domains that have been shown to influence processing efficiency result in a loss of the discrete subnucleolar domain, showing that this territory corresponds to a functional site of processing. Finally Rnt1p is found associated with the rDNA chromatin, showing that processing at the 3′ETS is a cotranscriptional event.

RESULTS

Rnt1pGFP strongly accumulates within a nucleolar structure different from the nucleolar body

To assess the subcellular localization of Rnt1p, we constructed a yeast strain in which the open reading frame (ORF) of the *RNT1* chromosomal gene is fused at the C terminus to the Green Fluorescent Protein (GFP; see Materials and Methods). In this strain, the expression of the sequence encoding the fusion protein is driven by the natural promoter and terminator sequences of *RNT1* and there are no auxotrophy markers present at the vicinity of the modified chromosomal region. Fluorescent microscopy analysis of cells expressing Rnt1p–GFP revealed that the fusion protein is only detectable in the nucleus and is not significantly observed in the cytoplasm, at least within the detection limits of our approach (Fig. 1A; data not shown). Some subnuclear accumulation could be observed, with a fraction of cells showing a nucleolar concentration of the GFP signal (Fig. 1A; data not shown). The GFP signal obtained with the protein expressed from its endogenous promoter was low, and required long exposure times (15–30 sec in Fig. 1A).

To facilitate localization studies and further study the protein domains required for its localization, we used a centromeric vector, pUG35 (Niedenthal et al. 1996) driving the expression of the Rnt1p–GFP fusion protein from a methionine conditional promoter (pUG35–RNT1). Yeast cells carrying a *RNT1* deletion were transformed with pUG35–RNT1, grown on plates lacking methionine and analyzed by fluorescence microscopy. The Rnt1p–GFP protein fusion fully complements the deletion of *RNT1*, as no detectable growth defect could be observed, neither on plates nor on liquid culture (data not shown). The GFP signal appeared similar to the one observed from the endogenous locus (Fig. 1A), but required much shorter exposure times for detection (1–2 sec). Therefore we decided to characterize the localization of Rnt1p in cells carrying the puG35–RNT1 plasmid. As described for the endogenous protein, Rnt1p–GFP expressed from the pUG35–RNT1 plasmid was found concentrated in a subnuclear structure in the majority of cells. This structure was not an artefact of fixation of the cells, as it could also be observed in living cells (data not shown). We characterized the localization of this structure using DAPI staining and the Nop1p protein as a nucleolar marker (Fig. 1B). The RNT1–GFP dots were observed at the periphery of the nucleus (Fig. 1B). This structure consistently overlaps with, or is juxtaposed next to the immunofluorescent signal corresponding to the endogenous Nop1p nucleolar protein (Fig. 1B). This dot-shaped nucleolar structure was reminiscent of a previously described subnucleolar domain, the nucleolar body (NB), that displays common characteristics with the Cajal Bodies observed in vertebrate cells (Verheggen et al. 2001).

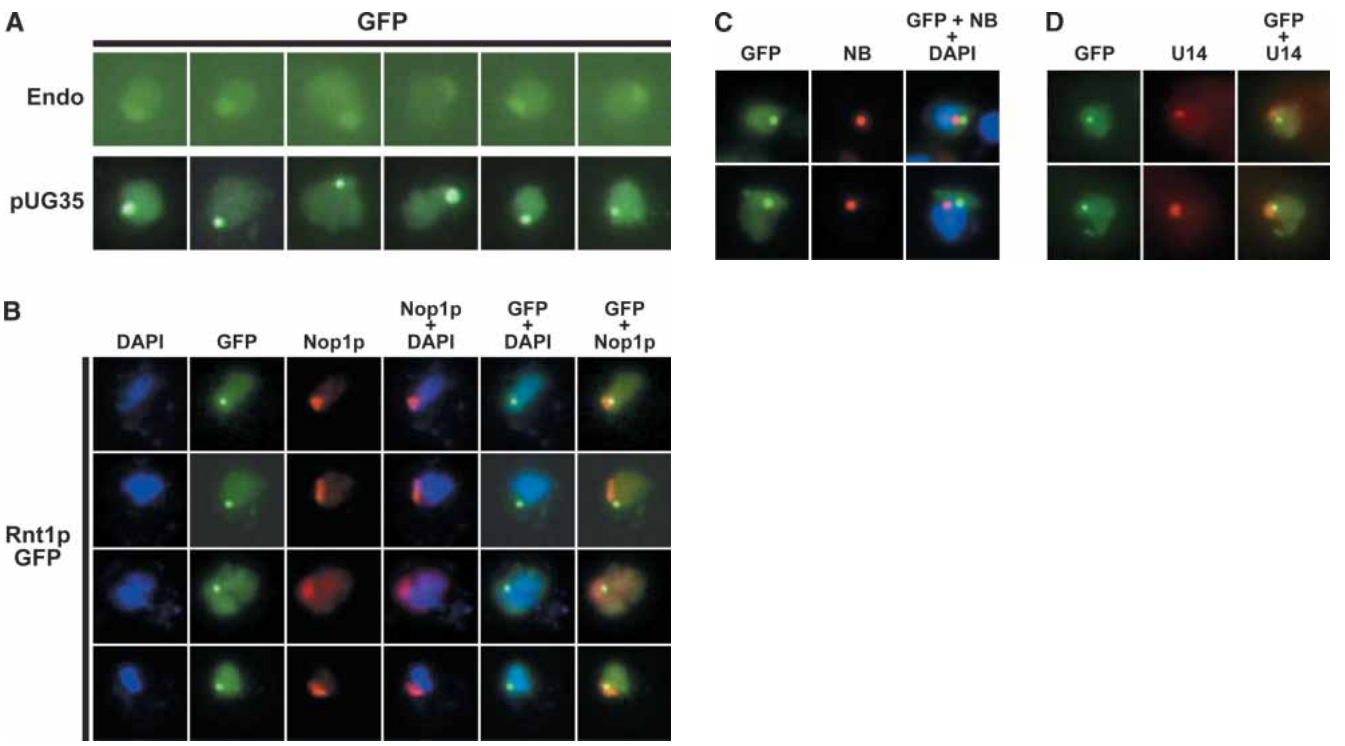

FIGURE 1. Rnt1p is localized in the nucleolus and in the nucleoplasm. (*A*) Subcellular localization of Rnt1p–GFP expressed from the endogenous locus (*top* row, endo) and from the pUG35 plasmid (pUG35). (*B*) Subcellular localization of Rnt1pGFP expressed from the pUG35 vector. Shown are pictures obtained from the haploid strain *rnt1*::*TRP* transformed with plasmids pUG35–RNT1, and treated for immunofluorescence with anti-Nop1p antibodies. From *left* to *right*, DAPI staining (blue), Rnt1p fused to the GFP (green), endogenous Nop1p (red), and merged images enabling the simultaneous visualization of both Nop1p and DAPI, GFP and DAPI, and Nop1p and GFP. (*C*) The nucleolar structure containing Rnt1p and the NB correspond to different nucleolar subdomains. (*Left*) Localization of Rnt1p–GFP (green); (*middle*) localization of the artificial snoRNA in the NB obtained by FISH (red); (*right*) merged image to which the DAPI staining has been added. (*D*) Rnt1p does not colocalize with the U14 snoRNA. (*Left*) Localization of Rnt1p–GFP (green); (*middle*) localization of the U14 snoRNA obtained by FISH (red); (*right*) merged image.

The NB has been proposed to be a discrete area of the nucleolus in which box C/D snoRNAs transiently accumulate before being targeted to their final functional sites. Some aspects of box C/D snoRNP biogenesis are thought to take place within the NB (Verheggen et al. 2001). Because Rnt1p participates in the maturation of many box C/D snoRNAs (Chanfreau et al. 1998a; Qu et al. 1999), we hypothesized that the nucleolar dot-shaped structure in which Rnt1p–GFP accumulates corresponds to the NB. To test this hypothesis, we simultaneously expressed Rnt1p–GFP and an artificial box C/D snoRNA that was previously shown to accumulate within the NB (Verheggen et al. 2001). Fluorescent in situ hybridization (FISH) using a probe complementary to this artificial snoRNA revealed that the nucleolar structure containing Rnt1p and the NB do not overlap (Fig. 1C), indicating that these two nucleolar subdomains correspond to distinct territories. In agreement with this observation, no change in the position or aspect of the Rnt1p–GFP signal were observed in a strain lacking Nsr1p or overexpressing Srp40p (data not shown), whereas the organization of the nucleolar body is affected in these strains (Verheggen et al. 2001). We conclude from these results that Rnt1p accumulates within a nucleolar subdomain that does not correspond to the nucleolar body.

The tRNA genes are found clustered in the nucleolus, where they colocalize with the U14 box C/D snoRNA (Thompson et al. 2003). This clustering is dependent upon efficient transcription by RNA polymerase I and is perturbed in a strain deprived of the nonessential RNA polymerase I subunit Rpa49p (Thompson et al. 2003). To investigate whether Rnt1p colocalizes with this nucleolar structure, we performed FISH experiments to detect the U14 snoRNA in a strain expressing Rnt1p–GFP. As shown in Figure 1D, the Rnt1p dot and U14 do not colocalize, showing that these correspond to distinct subnucleolar structures. This result is consistent with the position of the Rnt1p dot relative to Nop1p, a box C/D snoRNP component (Fig. 1). In addition, we introduced the pUG35–RNT1 plasmid in a *rpa49*Δ deletion strain, and we monitored the localization of Rnt1p–GFP. The Rnt1p dots were still detectable at 30°C in this mutant background strain (data not shown), showing that the Rnt1p dots do not correspond to the nucleolar territory where tRNA genes are clustered.

The 35S pre-ribosomal RNA is localized at the immediate periphery of the nucleolar territory where Rnt1p is concentrated

The primary ribosomal RNA transcript is the most highly expressed Rnt1p substrate in exponentially growing cells (60% of the cellular transcripts; Warner 1999). This precursor is produced by RNA polymerase I in the nucleolus and is thought to be rapidly processed by Rnt1p to generate the 35S pre-rRNA precursor (Allmang and Tollervey 1998; Reeder et al. 1999). The high amount of pre-rRNA precursor produced may require a high concentration of Rnt1p at the site of processing. Therefore, we hypothesized that the dot structure where Rnt1p accumulates corresponds to the region of the nucleolus where the enzyme takes part in the maturation of the rRNA precursor. To test this, we compared the localization of the endogenous 35S pre-rRNA with that of Rnt1p–GFP. This was achieved by FISH using a probe complementary to a region of the 5′ external transcribed spacer (5′ ETS), a flanking sequence not present in the mature rRNAs (Fig. 2A). This probe hybridizes upstream from the A0 site and detects only cleavage intermediates that contain the intact 5′ ETS, that is, the 35S precursor. As shown in Figure 2A, the the 35S pre-rRNA covers an area of the nucleolus whose shape is reminiscent of a pearl necklace, or is composed of discrete dots. The Rnt1p dot was always observed in very close proximity to the 35S, but the position of these two subnucleolar domains do not overlap. Significantly, on the images in which the FISH signal appears as a crown-shaped structure, the discrete focus containing Rnt1p is positioned in the middle of this structure. These observations suggest that the 35S pre-rRNA species that are generated by Rnt1p cleavage diffuse out from their initial site of processing, which can be visualized by the concentrated Rnt1p–GFP signal in the dot structure.

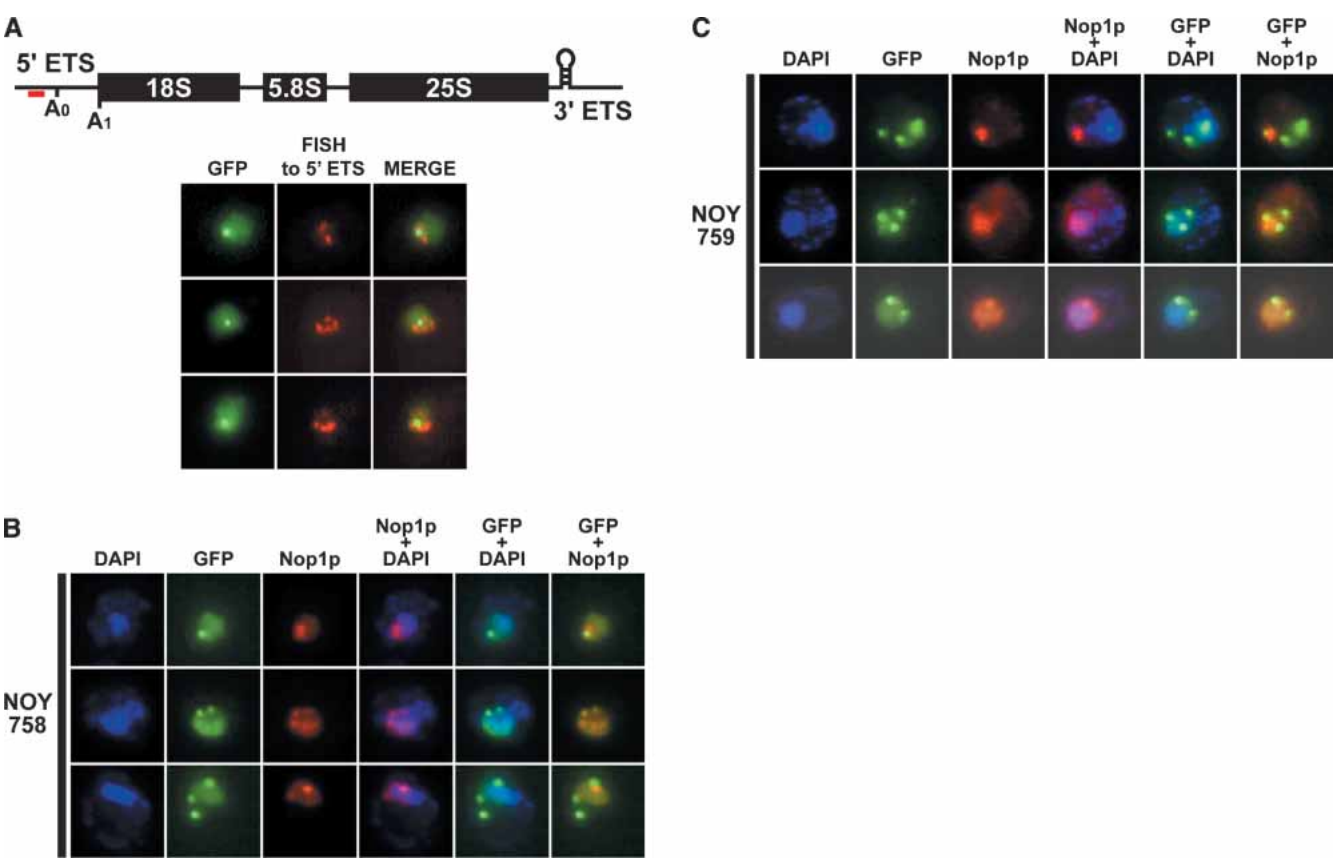

FIGURE 2. Localization of Rnt1p with the 35S pre-rRNA precursor and rDNA. (*A*) The 35S pre-rRNA is localized at the immediate periphery of the nucleolar dot containing Rnt1p. Shown is a schematic representation of the rRNA primary transcript. The red line indicates the site of hybridization of the oligonucleotide used in the FISH experiment. The hairpin indicates the site of Rnt1p cleavage. Shown are pictures obtained from the haploid *rnt1*::*TRP* strain transformed with plasmids pUG35–RNT1, and treated for pre-rRNA FISH. (*Left*) Rnt1p–GFP (green); (*middle*) localization of the 35S pre-rRNA (red); (*right*) merged image. (*B*) Rnt1p accumulates within several nuclear foci in a yeast mutant strain expressing the rRNAs from multicopy plasmids. Shown are (immuno)fluorescence pictures obtained from strain NOY758 transformed with pUG35–RNT1. Legends as in Figure 1A. (*C*) Rnt1p strongly accumulates within several nuclear foci in a yeast mutant strain expressing the rRNAs from multicopy plasmids containing an RNA polymerase II promoter. Shown are (immuno)fluorescence pictures obtained from strain NOY759 transformed with pUG35–RNT1. Legends as in Figure 1A.

The nucleolar subdomain containing Rnt1p corresponds to the territory in which the enzyme functions in the processing of the primary rRNA transcript

Transcription of the rDNA operon by RNA polymerase I results in the synthesis of a primary transcript whose 3′ end is extended approximately 210 nt past the 3′ end of the mature 25S rRNA (Reeder et al. 1999). This initial transcript, which contains the Rnt1p cleavage site, is not detectable by Northern blot in exponentially growing cells because it is rapidly converted by Rnt1p to the 35S precursor. This process may or may not be cotranscriptional (Allmang and Tollervey 1998; Reeder et al. 1999). If Rnt1p processing at the 3′ ETS occurs cotranscriptionally, Rnt1p should be found in a close vicinity of the ribosomal DNA. We thus speculated that the Rnt1p subnucleolar focus marks the position of the actively transcribed rDNA units. To test this, we tried to compare the localization the rDNA units by DNA FISH with the localization of Rnt1pGFP. This approach proved unsuccessful for technical reasons. The protocol used to hybridize a fluorescently labeled probe to the rDNA includes a proteinase K treatment aimed to degrade partially proteins associated with DNA. This treatment led to the degradation of the fusion protein and no GFP signal could be detected (data not shown). To circumvent this problem, we used two independent approaches to test whether Rnt1p is closely associated with the rDNA.

We first assessed the localization of Rnt1p in a yeast strain in which the expression of most of the ribosomal RNAs is driven by plasmid-borne rDNA units (NOY758, kindly provided by Prof. M. Nomura, Univ. of California, Irvine). In this strain, most of the chromosomal rDNA copies have been deleted and this lethal mutation is rescued by the introduction of a multicopy plasmid carrying a full rDNA unit controlled by its regular RNA polymerase I promoter (Oakes et al. 1998). Strains such as NOY758 have been shown to display a few (one to three) mini nucleoli that are believed to be organized around several gathered plasmids from which high amounts of primary ribosomal RNA transcripts emanate (Oakes et al. 1998; Trumtel et al. 2000). If Rnt1p accumulates at the sites of active rDNA transcription driven from these plasmids, we expected to observe multiple dots of Rnt1p–GFP. To test this hypothesis, we transformed the NOY758 strain with pUG35–RNT1, and analyzed Rnt1p–GFP localization by fluorescent microscopy. As expected, the GFP signal distribution was significantly different from the one observed in cells expressing the ribosomal RNAs from the endogenous chromosomal rDNA units. Depending on the cells, up to three Rnt1p–GFP dots could be observed (Fig. 2B; one dot: 60%; two dots: 18%; three dots or more: 5%; $n = 298$), whereas these multiple dot structures were never observed in the wild-type strain. The localization of the endogenous Nop1p protein was also modified in these particular cells. Instead of defining a single, large crescent-shaped area within the nucleus, several Nop1p-containing foci displaying different shapes and sizes could be observed in these mutant cells (Fig. 2B). These structures mark the territory of the nucleus devoted to the maturation of the pre-rRNAs in this mutant strain. Strikingly, most of the Rnt1pGFP foci are found at the immediate vicinity of a structure containing Nop1p. As previously described for wild-type cells, Rnt1p and Nop1p are found either juxtaposed or partially overlapping. This observation strongly suggests that these two areas of the nucleus correspond to distinct but physically linked regions. Importantly, some of the Rnt1p–GFP foci were observed in the cytoplasm (arrow in Fig. 2B). In these cases, Nop1p was absent from these structures. This observation strongly suggested that Rnt1p can associate with the site of transcription of the rDNA, independent from a nuclear localization. We propose that the Rnt1p-containing foci observed in these rDNA mutant cells precisely delimit the regions of the nucleus in which the plasmids supporting the expression of the pre-rRNAs are concentrated. This observation provides a first argument supporting the hypothesis that Rnt1p accumulates at the sites of transcription of the ribosomal DNA units.

To test whether Rnt1p colocalization with plasmid-borne rDNA units depends on RNA polymerase I, we used another strain in which the rRNAs are expressed from a different promoter. The NOY759 strain (kindly provided by M. Nomura) supports the synthesis of rRNAs from a multicopy plasmid in which rDNA units are under the control of a galactose-regulated, RNA polymerase-II-driven promoter (Oakes et al. 1998). In this strain, the nucleolus also appears fragmented (Oakes et al. 1998). To test whether Rnt1p remains associated with plasmid-borne rDNA units, we transformed NOY759 with the pUG35–RNT1, and assessed Rnt1p localization. In this strain, the fraction of cells in which the RNT1-GFP signal was fragmented was similar to that observed in the NOY758 strain (Fig. 2C; one dot: 53%; two dots: 18%; three dots or more: 8%; $n = 306$), indicating that the association of Rnt1p with the plasmid-borne rDNA units does not require the RNA polymerase I transcriptional machinery.

To prove unambiguously that Rnt1p is localized at the immediate vicinity of the rDNA units, we tested the association of Rnt1p with the rDNA chromatin using chromatin immunoprecipitation (ChIP) experiments. Yeast cells expressing Rnt1pGFP were grown in liquid culture to midlog phase and then treated with formaldehyde to induce the formation of covalent links between neighboring molecules. Cell extracts were subjected to the chromatin immunoprecipitation procedure (see Materials and Methods), and the DNA present in the final pellets was used as template in PCR reactions using different pairs of oligonucleotides. Figure 3 shows that Rnt1p is found associated with different regions of the rDNA such as the promoter region, the regions encoding a portion of the 5′ ETS, of the 25S rDNA,

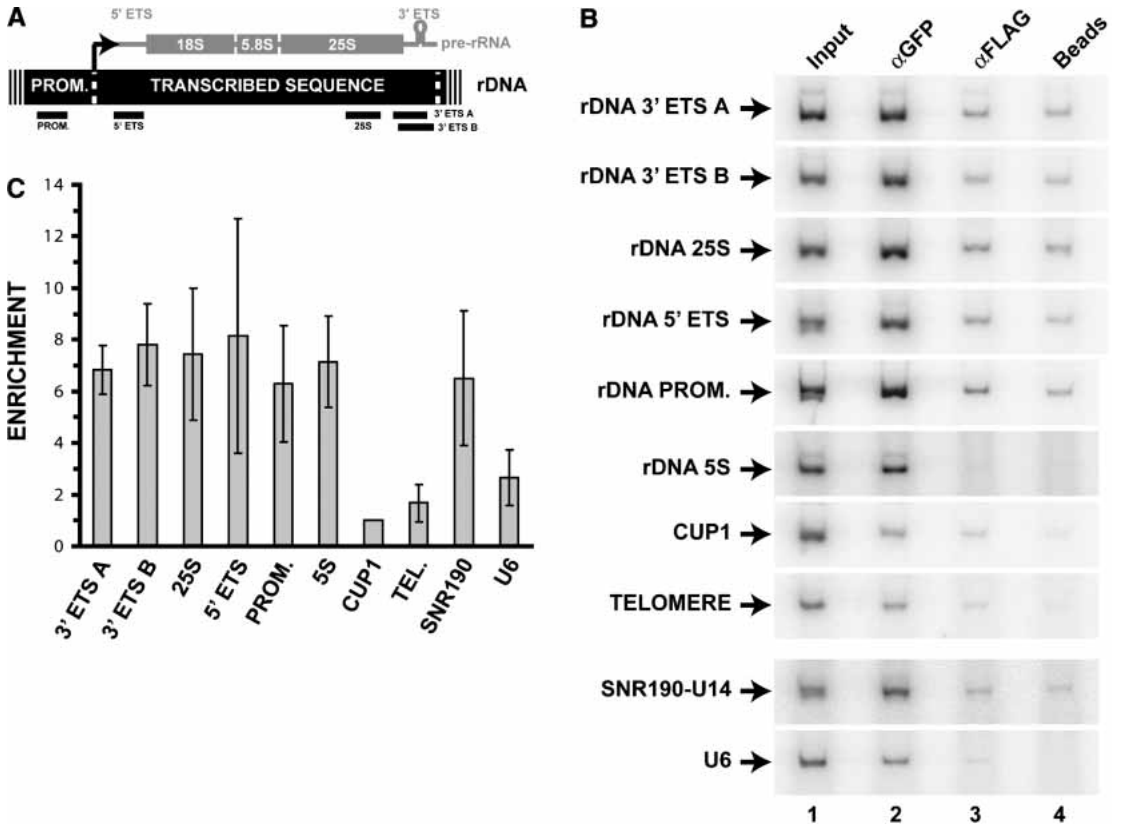

FIGURE 3. Rnt1p is associated with the rDNA chromatin. (*A*) Organization of the rDNA repeat and localization of the PCR products obtained in the ChIP procedure. (*B*) Shown are α^{32}P-labeled PCR products obtained from Input DNA (lane *1*) or DNA extracted from immunoprecipitation reactions in extracts prepared from the *rnt1:TRP*, pUG35–RNT1 strain using anti-GFP IgGs (αGFP, lane *2*), irrelevant anti-FLAG IgGs (α-FLAG, lane *3*), or with Protein G-conjugated sepharose beads only (Beads, lane *4*), using oligonucleotide pairs hybridizing to the indicated DNA sequences. (*C*) Quantification of the ChIP data. Five independent ChIP experiments were carried out as described in Materials and Methods. For each experiment, the intensity of the radioactive bands was measured using Image Quant. The relative immunoprecipitation efficiency of the different DNA targets by the anti-GFP antibodies was calculated as follows: For a given primer pair, the average intensity of the bands obtained in the negative control experiments and reflecting the immunoprecipitation background ("α-FLAG" or "Beads only" controls) was subtracted from the intensity of the band obtained with the relevant, α-GFP antibodies. The resulting value was then divided by the intensity of the band corresponding to the INPUT experiment. This value was then divided by the value obtained for the CUP1 signal (negative control). Error bars indicate the standard deviation. Because CUP1 was used as an internal standard for each experiment, no error bar is included.

and of two different regions of the 3′ ETS, as well as the 5S genes. The signals obtained after PCR in the anti-GFP immunoprecipitates were significantly higher than the signals obtained from the pellets obtained with the irrelevant anti-FLAG antibodies or with the protein G sepharose beads alone (compare the Input and IP lanes). In contrast, no enrichment was obtained in a strain expressing the GFP alone (data not shown). To test whether the association of Rnt1p with the rDNA is specific, and because the rDNA is repeated in multiple copies, we tested the interaction of Rnt1p with other repeated chromosomal regions. We chose the *CUP1* genes estimated to be present at a number of about 15–20 copies per haploid cells, and the telomeric DNA, present at both ends of each chromosome. The intensity of the signals corresponding to the different rDNA regions obtained with the anti-GFP immunoprecipitates represented between 65% and 75% (depending on the rDNA region) of the input signals. In the same conditions, the amplifications of a region of CUP1 and of a telomeric target gave signals representing only 10.75% or 16.5% of the input signals, respectively. These quantifications show that rDNA gene fragments are reproducibly found enriched four- to sevenfold in the Rnt1p–GFP immunoprecipitates compared to negative control regions such as the telomeres or the CUP1 genes. These results show that Rnt1p is associated with the rDNA chromatin, an observation fully consistent with the hypothesis that processing by Rnt1p at the 3′ ETS occurs cotranscriptionally.

The presence of Rnt1p at the vicinity of the 5S genes was somehow surprising because the 5S rRNA is not thought to be processed by Rnt1p. This enrichment could be explained by the tandem repetition of the rDNA repeats, where the 5S gene follows closely (0.8–1.2 kB) the preceding 25S sequence, and precedes closely the next rDNA promoter.

Given the low resolution of the ChIP technique and the tandem repeats organization of the yeast rDNA, the most straightforward explanation for the signal observed for the 5S rDNA is that it results from the presence of the Rnt1p protein 500 bp–1 kb upstream, near the 3′ ETS sequence. Nevertheless, to further prove the specificity of our chromatin immunoprecipitation reactions, we assessed the enrichment of Rnt1p near two other genes, the snR190-U14 snoRNA gene and the U6 gene. These genes were chosen because Rnt1p is known to process the dicistronic precursor that contains snR190 and U14 (Chanfreau et al. 1998b), but does not process U6. This ChIP experiment showed that Rnt1p is enriched near the snR190–U14 genes, but not at the vicinity of the U6 gene (Fig. 3), showing that chromatin immunoprecipitation using Rnt1p–GFP results in a selective enrichment of genes encoding Rnt1p substrates. This result also suggests that processing of the snR190–U14 precursor occurs in a cotranscriptional fashion.

The N-terminal domain of Rnt1p is not required for the import of Rnt1p into the nucleus but is necessary for formation of the nucleolar Rnt1p dot

The results presented so far indicate that Rnt1p is a nuclear enzyme distributed throughout the nucleus that also strongly accumulates within a nucleolar structure corresponding to the site of transcription of the rDNAs. We next focused on the identification of the domains of the protein required for this particular subcellular localization. We expressed truncated versions of Rnt1p fused to the GFP (Fig. 4A) and studied their localization. To define the boundaries of the truncations to be introduced in Rnt1p, we compared the amino acid sequence of Rnt1p with that of *Escherichia coli* RNase III. The bacterial enzyme is composed of an N-terminal catalytic domain containing the RNase III signature motif fused to a C-terminal dsRNA-binding domain. In Rnt1p, these two domains are flanked by two additional modules that are absent from the bacterial enzyme (Fig. 4A). The amino-terminal region of Rnt1p preceding the nuclease domain includes approximately 175 amino acids and was proposed to influence the dimerization of the enzyme (Lamontagne et al. 2000). Downstream from the dsRBD, the last 40 amino acids of Rnt1p define a carboxy-terminal domain that has been proposed to interact with Gar1p and to be required for the nuclear import of the box H/ACA snoRNP core proteins (Tremblay et al. 2002). These two domains are found specifically within the yeast enzyme and not in its bacterial counterpart. Thus, we suspected that in addition to their previously proposed function, they might play a role in the localization of the enzyme. We initially focused on the amino-terminal domain of Rnt1p because it had been proposed to be required for nuclear import (Nagel and Ares 2000). We studied the subcellular localization of two different truncated versions

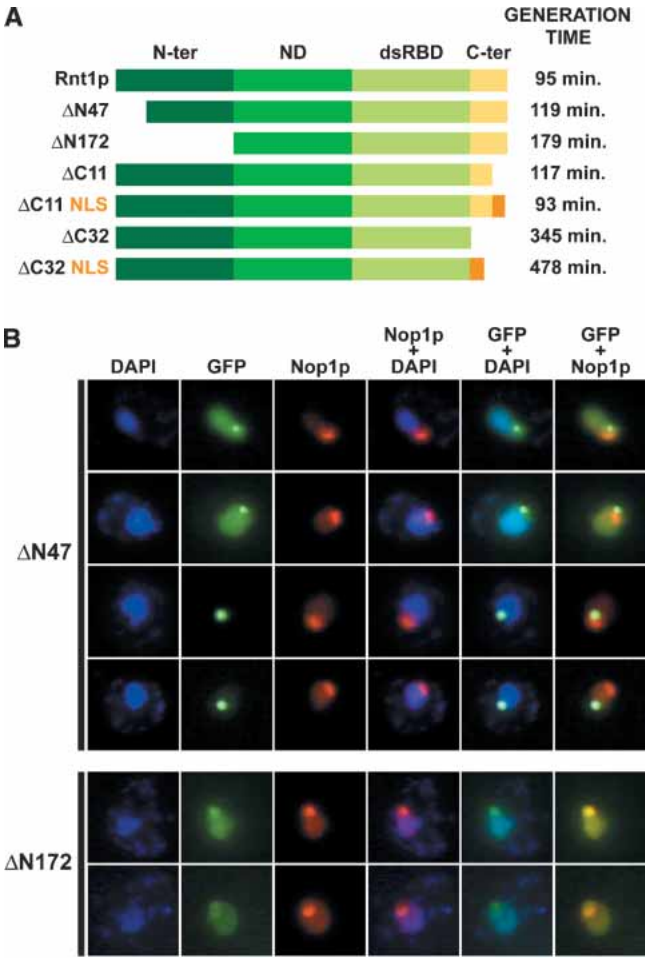

FIGURE 4. The N-terminal domain of Rnt1p is not required for the import of Rnt1p into the nucleus of yeast cells. (*A*) Schematic representation of the constructs used in the truncation analysis. Shown are the boundaries of the Rnt1p domains and of the truncations generated, and the generation time of the the *rnt1*::*TRP* transformed with the pUG35 derivatives expressing the different truncated versions of the protein. The generation time of *rnt1*::*TRP* transformed with plasmid pUG35 (knockout control) is 440 min. (N-ter) N-terminal domain, (ND) RNase III Nuclease Domain, (dsRBD) double-stranded RNA binding domain, (C-ter) C-terminal domain. (*B*) Shown are (immuno)fluorescence images obtained with the haploid strain *rnt1*::*TRP* transformed with plasmids pUG35–RNT1ΔN47 or pUG35–RNT1ΔN172. Legends as in Figure 1A.

of Rnt1p lacking the first 47 (Rnt1pΔN47) or 172 (Rnt1pΔN172) N-terminal amino acids. Yeast cells lacking the endogenous *RNT1* gene were transformed with pUG35-derivative constructs supporting the expression of these modified proteins fused to the GFP. The growth rate of the resulting strains and the localization of the modified proteins were assessed and compared to those of a strain in which the wild-type Rnt1p–GFP protein is expressed (Fig. 4).

Deletion of the first 47 amino acids of Rnt1p induced a significant growth defect, because Rnt1pΔN47 cells showed

a generation time approximately 20% longer than cells expressing the wild-type protein (Fig. 4A; the generation time of the wild-type equivalent, *rnt1::TRP* transformed with plasmid pUG35–RNT1 is 95 min). In the majority of these cells, the localization of Rnt1pΔN47 is comparable to the localization of the wild-type Rnt1p (Fig. 4B, upper panels). Interestingly, we observed that in a significant fraction of cells (23.5%, $n = 570$), Rnt1pΔN47 displays a very different localization pattern (Fig. 4B, lower panels). In these cells, the GFP signal is still only detectable within the nucleus, but appears concentrated within a single, large dot-shaped structure whose nuclear position is variable depending on the cell. Such structures could be observed within the nucleolus, the nucleoplasm, or at the interface between these two subnuclear areas (Fig. 4B; data not shown). These observations indicate that the deletion of the 47 N-terminal amino acids of Rnt1p affects the localization of the enzyme in a cell-specific manner, because the modified protein appears normally localized in the majority of the cells but is aberrantly concentrated, and perhaps aggregated within a single nuclear structure in a subset of cells. The reasons for this cell-specific localization defects remain obscure. This may reflect a difference in the level of expression of the modified protein in individual cells or, alternatively, a different stage of the cell cycle in which the cells are engaged.

Yeast cells expressing a modified version of Rnt1p lacking its entire N-terminal domain (Rnt1pΔN172) displayed a severe growth defect (Fig. 4A), consistent with previous studies (Lamontagne et al. 2000; Nagel and Ares 2000). Analysis of the subcellular localization of the truncated protein revealed that the protein is still exclusively nuclear (Fig. 4B). Within the nucleus however, the localization pattern significantly differed from the one observed for the full-length protein. In 88% of the cells ($n = 221$), the modified protein displayed a homogenous nuclear distribution, without significant accumulation in any subregion of this compartment. In the other 12%, the modified protein appears distributed throughout the nucleus and over-accumulated within a subnuclear area partially overlapping with the nucleolus. The main difference between the localization of the Rnt1pΔN172 and the wild-type protein consists in the fact that the discrete dot-shaped subnucleolar structure is not present in cells expressing the truncated enzyme. Instead, a more diffuse signal localized in the region of the nucleolus is sometimes observed in a small subset of cells. Two main conclusions can be inferred from these localization data. First, whatever the function of the N-terminal domain of Rnt1p, it is not required for the nuclear import of the enzyme, because the Rnt1pΔN172 truncated version of Rnt1p still accumulates within the nucleus. Second, the absence of the N-terminal domain of Rnt1p affects the structure and/or function of the protein in such a way that the enzyme loses its ability to strongly concentrate in the nucleolus at the site of transcription of the rDNAs.

The extreme C-terminal domain of Rnt1p contains a nuclear localization signal (NLS) and a functionally important domain for visualization of the Rnt1p foci

The last 40 amino acids of Rnt1p define a C-terminal domain of the yeast enzyme that is not present in *E. coli* RNase III. This C-terminal domain contains a cluster of five positively charged amino acids out of six residues (KNKKRK), preceded by a 20-amino-acid region containing several scattered lysine and arginine residues positioned close to each other. The sequence of this domain is very similar to the organization of known NLS motifs, which present a high content in positively charged amino acids such as lysine and arginine residues (Dingwall and Laskey 1991). These residues can either be present as a single cluster, such as within the SV40 large T antigen NLS, or define two clusters separated by a short spacer region to form a bipartite NLS motif. To determine whether the C-terminal domain governs the nuclear import of Rnt1p, we introduced different deletions within this region (Fig. 4A) and expressed the modified proteins in yeast cells lacking endogenous Rnt1p. We then assessed the effect of the different truncations on cell growth and on the subcellular localization of Rnt1p (Fig. 5A). Deletion of the last 11 amino acids of Rnt1p including the cluster of five basic amino acids induces a significant growth defect because cells expressing the modified protein, Rnt1pΔC11-GFP, display a generation time approximately 20% longer than cells expressing the wild-type protein (Fig. 4A). Figure 5A shows that this truncation leads to a defect in the nuclear import of Rnt1p. A large fraction of the GFP signal indeed accumulated in the cytoplasm, indicating that Rnt1pΔC11-GFP is not efficiently imported in the nucleus. This import defect is only moderate because a significant GFP signal is observed in the nuclear compartment. Seventy-five percent of cells showed a homogenous cytoplasmic and nuclear localization, whereas 24% showed a slight nuclear exclusion ($n = 215$). A very low percentage (<1%) of cells display a nuclear GFP signal comparable to the one observed with the wild-type protein, although the signal is much weaker (Fig. 5A, lower panel). We conclude from these observations that the last 11 amino acids of Rnt1p are required for an efficient import of the enzyme into the nucleus. To determine whether the phenotypes induced by the expression of Rnt1pΔC11 only originates from an inefficient import of the enzyme, we fused this truncated protein to the SV40 nuclear targeting sequence, a NLS shown to function efficiently in yeast. Interestingly, cells expressing this new construct (Rnt1pΔC11NLS) displayed a growth rate identical to the one of cells containing the wild-type protein (Fig. 5A). In agreement with this result, the observed localization pattern of Rnt1pΔC11NLS is very similar to the one of the unmodified Rnt1p (Fig. 5A). Eighty-six percent of cells show a wild-type dot structure, whereas 14% show a homogenous nuclear localization with no nucleolar accumulation ($n = 213$). These results strongly

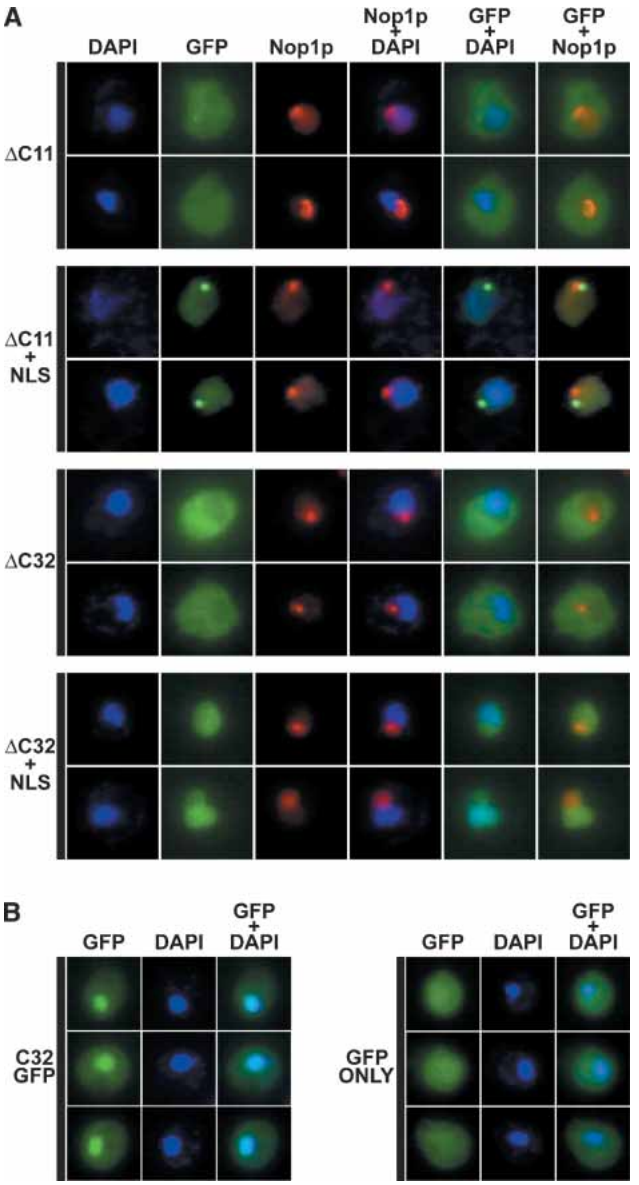

FIGURE 5. The C-terminal domain of Rnt1p is necessary and sufficient for nuclear import. (*A*) Deletion of the C-terminal amino acids of Rnt1p perturbs nuclear import. Shown are (immuno)fluorescence images obtained with the haploid strain *rnt1::TRP* transformed with plasmids pUG35–RNT1ΔC11, pUG35–RNT1ΔC11NLS, pUG35–RNT1ΔC32, or pUG35–RNT1ΔC32NLS. Legends as in Figure 1A.(*B*) The C-terminal domain of Rnt1p is a bona fide nuclear targeting signal. Shown are fluorescence pictures obtained from the haploid strain BMA64 (wild type) transformed with plasmid pUG35-C32 or pUG35.

suggest that the last 11 amino acids of Rnt1p only take part in the import of the enzyme but are not involved in any aspect of its nuclear functions.

Deletion of the last 11 amino acids of Rnt1p only partially affects the import of Rnt1p, suggesting that this region of the protein is part of a larger NLS. To test this hypothesis, we deleted the last 32 amino acids and analyzed the effects of this truncation. A yeast strain expressing Rnt1pΔC32 displayed a severe growth defect, as its growth rate is reduced by almost four times compared to the wild-type control and it grew only slightly faster than the knockout strain (Fig. 4A). The last 32 amino acids of Rnt1p are therefore almost essential for the function of the enzyme. Analysis of the subcellular localization of Rnt1pΔC32–GFP revealed a strong defect in the nuclear import of the truncated protein (Fig. 5A). Thirty-three percent of cells ($n = 30$) showed a homogenous nuclear and cytoplasmic GFP signal, whereas 67% showed a slight to strong nuclear exclusion, indicating a very low concentration of Rnt1pΔC32 in the nucleus. The last 32 C-terminal amino acids of Rnt1p therefore define a domain that is essential for the nuclear import of Rnt1p. Expression of Rnt1pΔC32 fused to the SV40 NLS did not abolish the growth defect observed with the truncated protein. The growth rate was, on the contrary, further reduced, the generation time of this strain being increased by five times compared to the wild-type control. Surprisingly, this strain grew slower than the knockout strain (Fig. 4A), indicating that the expression of Rnt1pΔC32NLS is more deleterious than the absence of Rnt1p. However this protein did not exhibit a dominant negative effect when expressed in wild-type cells (data not shown). The Rnt1pΔC32NLS protein was present within the nucleus, as expected given the presence of the SV40 NLS. The distribution of the enzyme inside the nucleus is, however, different from the distribution of the wild-type protein. Rnt1pΔC32NLS was homogenously distributed throughout the nucleus, without significant accumulation in any subnuclear domain. We conclude that the last 32 amino acids of Rnt1p, in addition to being essential to the import of the enzyme, also include residues that are required for the discrete accumulation of Rnt1p at the site of transcription of the rDNAs. It is possible that the deletion of the whole C-terminal domain of Rnt1p alters the structure of the double-stranded RNA-binding domain located nearby (Wu et al. 2004) and decreases RNA binding, preventing Rnt1p accumulation into functional sites.

The previous results show that the C-terminal domain of Rnt1p includes a motif that is necessary for the import of the protein into the nucleus. To match the definition of an NLS, this domain must also be sufficient to direct a non-nuclear protein to the nucleus. To determine whether the C-terminal domain of Rnt1p displays such a property, we fused the last 32 amino acids of Rnt1p to the GFP and compared the localization of this construct to the localization of the GFP alone in wild-type yeast cells. As shown in Figure 5B, when fused to the C-terminal domain of Rnt1p, the GFP moiety became predominantly localized in the nucleus compared to the GFP alone, which localizes uniformly in the cell. These results demonstrate that the C-terminal domain of Rnt1p is both necessary and sufficient to govern the active import of a protein into the nucleus and hence behaves as a bona fide nuclear targeting signal. Finally, deletion of Rnt1p domains that are required for

efficient RNA processing results in a loss of accumulation in the dot-shaped territory, suggesting that this territory corresponds to a functional site of processing.

DISCUSSION

Analysis of Rnt1p localization

In this study we have shown that Rnt1p can be found localized in the nucleus of yeast cells, with a diffuse nucleoplasmic and nucleolar signal and a very discrete localization pattern in a dot-shaped structure. This dot-shaped structure is adjacent to the nucleolus, because the Nop1p and the Rnt1p signals are juxtaposed. This structure is distinct from the nucleolar body (Fig. 1B). Significantly, the 35S pre-rRNA is organized at the periphery of this dot-shaped structure, suggesting that the dot-shaped Rnt1p territory corresponds to the site of processing of the rRNA primary transcript, from which the 35S pre-rRNAs diffuse.

The localization pattern that we have described differs somewhat from the Rnt1p localization pattern described in two other studies (Huh et al. 2003; Catala et al. 2004). These studies show that Rnt1p localizes in the nucleus and the nucleolus, but they could not detect the dot-shaped territory that we describe. We have noticed that the Rnt1p foci can be clearly visualized when yeast cells are grown from plates, but they are very rarely seen when cells are grown in liquid cultures (data not shown). This situation is reminiscent of the nucleolar body, which can be visualized much more easily when cells are grown on solid medium (Verheggen et al. 2001). Thus the growth conditions used in these studies may have hampered the visualization of subcellular territories.

We have determined the Rnt1p domains that are required for proper localization. Several Rnt1p truncations have been described previously (Lamontagne et al. 2000; Nagel and Ares 2000; Tremblay et al. 2002). Phenotypic analysis revealed that the N- and C-terminal domains of Rnt1p are required for optimal processing in vivo (Lamontagne et al. 2000; Nagel and Ares 2000; Tremblay et al. 2002), but these studies did not include the analysis of the effect of these truncations on Rnt1p localization. We show that Rnt1p import in the nucleus requires a nuclear localization signal found in the last 32 amino acids of the protein. The requirement of the C terminus of Rnt1p for nuclear import was also demonstrated in a recent study (Catala et al. 2004). The C terminus of Rnt1p has similarities with classical importin α-type NLS, so it is reasonable to believe that import occurs through a classical importin α pathway. This assumption is strengthened by proteomics studies showing that Rnt1p interacts with Srp1p, the *S. cerevisiae* ortholog of importin α (Ito et al. 2001; Ho et al. 2002). Alternatively, it is possible that Rnt1p nuclear import through the C-terminal domain requires alternative import pathways. The C-terminal domain responsible for Rnt1p import also maps to a site of interaction with a box H/ACA snoRNP core protein, Gar1p (Tremblay et al. 2002). Thus it is possible that Rnt1p nuclear import may depend on an efficient interaction with Gar1p. However, the fact that the nuclear import defect induced by the deletion of the last 11 or 32 amino acids of Rnt1p is efficiently relieved by addition of the SV40 NLS suggests that nuclear import of Rnt1p follows a classical NLS pathway. The observation that the Rnt1pΔC32–NLS construct is homogenously distributed throughout the nuclear area, without noticeable accumulation in any subnuclear domain, is consistent with the fact that both the function and the nuclear import of the protein require the last 32 amino acids. The fact that the Rnt1p foci cannot be observed in this strain suggests that the loss of functionality in the enzyme results in a loss of the foci, showing that these foci correspond to functional processing sites. These results identify two independent functions for the C-terminal domain of Rnt1p: (1) nuclear import of the protein and (2) proper intranuclear distribution, possibly through proper function.

The N-terminal domain, which is not found in prokaryotes, had been proposed to be required for nuclear import (Nagel and Ares 2000). Our results show that this domain does not seem to be involved in localization per se. Deletion of the first 172 amino acids of the protein does not perturb nuclear import, but results in a disappearance of the dot-shaped structure. The absence of this domain has been shown to affect the function of Rnt1p by interfering with the dimerization of the enzyme (Lamontagne et al. 2000). In addition, deletion of this domain affects RNA processing efficiency in vivo, in particular processing of the 3′ ETS (Lamontagne et al. 2000; Nagel and Ares 2000). The loss of the dot-shaped structure observed in strains expressing the Rnt1pΔN172 construct shows that the Rnt1p foci correspond to functional RNA processing sites. A dimerization defect or any functional RNA cleavage defect may affect the ability of the protein to concentrate at processing sites, especially at the site of transcription of the rDNAs.

A cotranscriptional model for pre-rRNA processing at the 3′ external transcribed spacer

Previous studies have suggested that processing of the rRNA precursor is somehow coupled to transcription or occurs very rapidly after transcription. First, the primary yeast pre-rRNA transcript is hardly detectable in vivo (Allmang and Tollervey 1998; Reeder et al. 1999), suggesting that Rnt1p cleavage is cotranscriptional or follows transcription very rapidly. Reciprocally, a recent report showed that termination of transcription of the rDNA is affected by depletion of Rnt1p (Prescott et al. 2004), suggesting a feedback mechanism between cleavage at the 3′ ETS and termination of transcription. Several studies have suggested a direct link between other pre-rRNA processing factors and RNA polymerase I. The U14 and U3 snoRNAs and the H/ACA

snoRNP protein Gar1p localize in the dense fibrillar component (Lazdins et al. 1997; Leger-Silvestre et al. 1999), the probable site of transcription by RNA polymerase I (Hozak et al. 1994; Jackson and Cook 1995; Lazdins et al. 1997; Mosgoeller et al. 1998). In addition, the nucleolar processing factor Nop1p colocalizes with RNA polymerase I in mouse embryos (Cuadros-Fernandez and Esponda 1996) and with nascent rRNA transcripts (Garcia-Blanco et al. 1995). In addition, several snoRNP proteins and rRNA processing factors can be found biochemically associated with yeast RNA polymerase I (Fath et al. 2000). These observations have linked pre-rRNA processing to RNA polymerase I transcription. Our results strongly suggest that in *S. cerevisiae*, cleavage of the primary pre-rRNA transcript by Rnt1p to generate the 35S precursor is a cotranscriptional event. Because the transcription of the rDNA genes represents about 60% of the total cellular transcription (Warner 1999), high amounts of primary ribosomal RNAs continuously emerge from the active rDNA units, and their 3′-end processing is likely to mobilize high amounts of Rnt1p. The chromatin immunoprecipitation results (Fig. 3), and the fact that the dot-shaped Rnt1p territory becomes reorganized when the rRNAs are expressed from multicopy plasmids provide evidence for association of Rnt1p with rDNA units. In the light of these considerations, we conclude that the observed nucleolar area in which Rnt1p is strongly accumulated corresponds to the site of transcription of the rDNA genes and early processing of the ribosomal RNA precursor. In support of this hypothesis, it was recently shown that the nucleolar accumulation of Rnt1p is reduced in a polymerase I temperature-sensitive strain (Catala et al. 2004). However, analysis of Rnt1p localization in a *rpa49*Δ strain, in which the levels of transcription by RNA polymerase I are reduced (Liljelund et al. 1992), did not show a significant difference compared to wild-type cells (data not shown). Interestingly the reorganization of the Rnt1p foci around plasmid-borne rDNA units occurs even if the rRNAs are expressed from an RNA polymerase II promoter (Fig. 2C). This suggests that Rnt1p association with the rDNA may occur independently from the specific RNA polymerase machinery, or that Rnt1p may be recruited by a subunit of the polymerase that is common between RNA polymerases I and II. Intriguingly, there is no significant enrichment of Rnt1p at the vicinity of the 3′ ETS rDNA region compared to other rDNA regions in our ChIP experiment, showing that Rnt1p is probably evenly distributed throughout most of the rDNA region. Alternatively, it is possible that the repeated nature of these sequences makes local enrichment very hard to distinguish using the chromatin immunoprecipitation technique. For example, the enrichment observed in the 5S region may be due to the close proximity of this sequence to the preceding 3′ ETS and to the poor resolution of the ChIP technique. The even distribution of Rnt1p throughout the rDNA can suggest several models of cotranscriptional cleavage of the pre-rRNA transcript. In the first model, Rnt1p is present statically on most regions of the rDNA, but the fraction of Rnt1p present at the vicinity of the 3′ ETS sequence at the DNA level may be sufficient to cleave the nascent 3′ ETS sequence after this sequence exits from the RNA polymerase. Alternatively it is possible that the Rnt1p subunits present along the rDNA may form a reservoir of enzymes. In this model, the RNA polymerase machinery (through a subunit that would be common to Pol I and Pol II) would recruit one of the Rnt1p subunits present in the chromatin when it travels along the rDNA transcription unit. Finally it is possible that Rnt1p is recruited very early at the promoter by the RNA polymerase, and that it travels along the rDNA unit with the RNA polymerase. The presence of Rnt1p along the entire rDNA sequence observed by chromatin immunoprecipitation would result from the dynamic association of Rnt1p with the RNA polymerase machinery. Further experiments may shed light on the validity of each of these models.

MATERIALS AND METHODS

Yeast strains and plasmids

Yeast manipulation and transformation was performed using standard techniques. The sequence of oligonucleotides used is available upon request. Most yeast strains used in this study are a derivative of BMA64 (Baudin et al. 1993). Yeast strains carrying the *rnt:TRP* disruption have been described previously (Chanfreau et al. 1998b). The NOY758 and NOY759 strains were kindly provided by M. Nomura (Oakes et al. 1998). The *rpa49*Δ strain was purchased from Open Biosystems. To construct plasmids expressing the RNT1–GFP fusions, the *RNT1* open reading frame was amplified by PCR using *Pfu* Polymerase (Stratagene) and cloned into pUG35 (Niedenthal et al. 1996), using BamHI and ClaI sites that were introduced into the primers used for PCR. Truncations in the *RNT1* gene were generated by PCR. For construction of the strain carrying a GFP fusion at the endogenous *RNT1* locus, a Kan-URA marker was first inserted after the *RNT1* stop codon, as described (Storici et al. 2001). A PCR fragment was generated using the pUG35–RNT1 plasmid as a template, an upstream oligonucleotide hybridizing from positions 620–640 of the *RNT1* ORF, and a downstream oligonucleotide hybrdizing to the end of the GFP sequence. The downstream oligonucleotides also carried 50 nt of complementarity to the RNT1 3′ UTR. In a second step, this PCR fragment was transformed in the previously described strain, and transformants were selected on 5-fluoroorotic acid, and screened for correct insertion of the GFP fusion by PCR on yeast colonies.

Indirect immunofluorescence microscopy

Cells were collected from patches grown on plates and transferred to small Erlenmeyer flasks containing 10.5 mL of liquid medium (same composition as the medium corresponding to the initial plates). Cells were fixed by adding 1.5 mL of 16% formaldehyde

(2% final concentration) and incubating for 30 min at 30°C with gentle shaking. Cells were washed once with 1 mL of 0.1 M KPO_4 (pH 6.5) and once with 1 mL P solution (1.2 M Sorbitol in 0.1 M KPO_4 at pH 6.5). Cell were pelleted and resuspended with 1 mL of P solution. Spheroplasts were generated by adding 15 µL of 10 mg/mL Zymolyase 20T (Seikagaku Corp.) and 5 µL of β-mercaptoethanol, and incubated for 1 h at 37°C with gentle shaking. Spheroplasts were recovered by gentle centrifugation, resuspended with 500 µL of P solution, and spotted on eight-well multitest slides previously coated with polylysin. After 10 min, excess cells were removed and the slides were incubated for 6 min in ice-cold methanol followed by 30 sec in ice-cold acetone. Slides were then washed twice with 5 mg/mL BSA, 1× PBS and incubated for 2 h at room temperature with anti-Nop1p monoclonal antibodies (kindly provided by J. Aris, Univ. of Florida) diluted 1:5000 in 5 mg/mL BSA in 1× PBS. Slides were then washed three times for 5 min with 5 mg/mL BSA in 1× PBS and incubated for 2 h at room temperature with Cy3-conjugated anti-mouse IgGs (Sigma) diluted 1:1000 in 5 mg/mL BSA, 1× PBS. Slides were then washed three times with 1× PBS, incubated for 10 min at room temperature with 4,6-diamidino-2-phenylindole (DAPI) diluted to 1 µg/mL in 1× PBS. Slides were washed three times for 5 min with 1× PBS and covered with 60% glycerol and a coverslip. Fluorescent images were captured with an Optronics cooled CCD camera attached to a Zeiss Axioplan microscope. All images were captured with a PHOTOSHOP AV capture plug-in on a Macintosh Power PC AV computer.

Fluorescent in situ hybridization (FISH)

Detection of the nucleolar body by FISH was performed as described (Verheggen et al. 2001). FISH detection of the 35S pre-rRNAs was performed as follows, using the probe 5′AX CCTTCGCTGCXCACCAATGGAAXCGCAAGATGCCCACGAXG′ (X = Cy3-dT). This probe hybridizes upstream of the A0 site.

FISH detection of the U14 snoRNA was performed as follows using a mixture of the two following probes: 5′Cy3-GTGGAAAC TGCGAAT GTT AAG GAAC CAGTC TTTCATCACCGTGAT-Cy3 and 5′Cy3-GAAGAGCGGTCACCGAGAGTACTAACGATGGGTT CGTAAGCG-Cy3. Cells were collected from patches grown on plates and transferred to small Erlenmeyer flasks containing 9 mL of liquid medium (same composition as the medium corresponding to the initial plates). Cells were fixed by adding 3 mL of 16% formaldehyde (4% final concentration) and incubated for 30 min at 25°C with gentle shaking. Cells were then recovered and washed once with 10 mL of buffer B (1.2 M sorbitol, 100 mM K-phosphate buffer at pH 7.5). Cells were recovered by centrifugation, resuspended with 500 µL of digestion buffer (1 mL of Buffer B, 20 µL of 50× Complete EDTA-free protease inhibitor cocktail [Roche Diagnostics], 10 µL of 200 mM vanadium ribonucleoside complex, 2 µL of PMSF, 2 µL of β-mercaptoethanol, 10 µL of 20 mg/mL Zymolyase 20T from Seikagaku dissolved in buffer B) and incubated for 30 min at 30°C with gentle shaking. After digestion, spheroplasts were recovered by centrifugation, rinsed with 10 mL of ice-cold buffer B, pelleted again, and resuspended with 300 µL of ice-cold buffer B. Aliquot fractions of the suspension (50 µL) were spotted on each well of a multitest slide previously coated with polylysin. After incubation for 30 min, excess cells were removed and the slide was incubated overnight in −20°C 70% ethanol. Spheroplasts were then rehydrated by incubating the slide twice for 5 min with 2× SSC at room temperature and for 5 min with 2× SSC, 10% formamide.

For the in situ hybridization of the probe to the spheroplasts, two different solutions (A and B) were prepared separately. Solution A was obtained by mixing 2 µL of a 10 ng/µL oligonucleotide probe solution, 4 µL of formamide, 2 µL of 2× SSC, 2 µL of 10 mg/mL wheat germ tRNAs, and 7 µL of ddH_2O. Solution B was obtained by mixing 20 µL of 20% dextran sulfate in 4× SSC, 2 µL of 10 mg/mL BSA, and 2 µL of 200 mM vanadium ribonucleoside complex. Solution A was incubated for 5 min at 100°C, chilled on ice for 5 min, and mixed with room temperature solution B. The resulting solution was loaded onto the slide (20 µL per well) and incubated for 3 h at 37°C. Slides were then washed two times for 15 min at 37°C with 37°C pre-warmed 2× SSC, 10% formamide one time for 15 min at room temperature with 2× SSC, 0.1% Triton X-100 and then two times for 15 min at room temperature with 1× SSC. Slides where then rinsed three times for 5 min with 1× PBS at room temperature, incubated for 10 min with a 1 µg/mL DAPI solution at room temperature, and rinsed again three times for 5 min with 1× PBS. Slides were covered with 60% glycerol and a coverslip, and imaging was performed as described above.

Chromatin immunoprecipitation (ChIP)

A 50-mL culture of the relevant yeast strain was grown to a late exponential phase ($OD_{600} = 1$). Cross-linking was achieved by adding formaldehyde to the culture to a final concentration of 1% and incubating for 30 min at 30°C with gentle shaking. Cross-linking was quenched by adding glycine to a final concentration of 125 mM and incubating for 5 min at 30°C with gentle shaking. Cells were transferred into a 50-mL centrifugation tube, washed twice with 20 mL ice-cold 1× PBS, and transferred into 1.5-mL siliconized tubes. After centrifugation, cell pellets were resuspended with 400 µL ice-cold lysis buffer (50 mM HEPES/KOH at pH 7.5, 500 mM NaCl, 1 mM EDTA at pH 8.0, 1% Triton X-100, 0.1% sodium-deoxycholate, 0.1% SDS) supplemented with protease inhibitors (Complete EDTA-free; Roche Diagnostics). Glass beads (500 µL) were added to the tubes and cells were broken by vigorous vortexing for 45 min at 4°C. Extract and cell debris were separated from the beads and sonicated on ice two times for 15 sec (sonic Dismembrator 550, Fisher Scientific, setting 4 out of 10), with a 1-min interval. Cell debris was pelleted by centrifugation (13,000 rpm, 5 min, 4°C) and the supernatant was recovered and transferred to a new 1.5-mL siliconized tube. A 20-µL aliquot fraction of this extract was frozen at this stage for subsequent analysis (INPUT; see below).

Each immunoprecipitation (IP) experiment was carried out using a 50-µL aliquot fraction of the extract transferred to a new 1.5-mL siliconized tube. We added 1.5 µg of anti-GFP antibody (Clontech), 1.5 µg of an irrelevant antibody, or no antibody to a 50-µL aliquot fraction of extract and incubated overnight at 4°C with gentle shaking. Recovery of the antibodies and their bound epitopes was achieved by adding to each tube 25 µL of a 50% protein-G sepharose beads (Pharmacia) suspension (1 volume of bead:1 volume of lysis buffer; beads were previously washed several times with ddH_2O and then twice with the Lysis Buffer), incubating 90 min at 4°C with gentle shaking and spinning at 2000 rpm for 2 min at 4°C. Beads pellets were then washed two times for 10 min with 1 mL of lysis buffer at 4°C, one time for 10 min with 1 mL of sodium-deoxycholate buffer (10 mM Tris-HCl at pH

8.0, 0.25 M LiCl, 0.5% NP-40, 0.5% sodium-deoxycholate, 1 mM EDTA at pH 8.0) at 4°C and one time for 10 min with TE (10 mM Tris-HCl at pH 8.0, 1 mM EDTA at pH 8.0) at 4°C. After the last wash, beads were pelleted and the washing buffer was removed completely.

Immunoprecipitated proteins were eluted from the beads and the cross-link was reversed by mixing bead pellets with 50 µL of elution buffer (50 mM Tris-HCl at pH 8.0, 10 mM EDTA at pH 8.0, 1% SDS) and incubating overnight at 65°C in a hybridization oven. At this stage, the 20-µL INPUT aliquot fractions were thawed, mixed with 80 µL of TE, and incubated along with the immunoprecipitates. Eluates were recovered from the IP experiments (about 50 µL) and diluted by adding 50 µL of TE. A 1:10 aliquot fraction (10 µL) was taken out at this stage, mixed with SDS-loading buffer, and frozen for subsequent Western blot analysis of the precipitated proteins. We added 10 µg of glycogen and 100 µg of proteinase K to the remaining samples and tubes were incubated for 2 h at 56°C. DNA fragments contained in the IPs and INPUTs were purified by phenol extraction followed by ethanol precipitation and the final DNA pellets were resuspended with 40 µL of ddH_2O. Contaminant RNA molecules potentially present in the samples were degraded by RNase A treatment. PCR reactions were carried out using 0.5 µL of the immunoprecipitated DNAs or 0.5 µL of a 1:100 dilution of the INPUT DNAs, with Pfu Turbo polymerase (Stratagene) and in the presence of 1 µCi of α^{32}P dCTP per reaction. Half of the PCR reactions were mixed with loading buffer and loaded on 6% acrylamide:bisacrylamide (19:1), 0.5× TBE gels. After migration, gels were dried and exposed to PhosphorImager screens.

ACKNOWLEDGMENTS

We thank J. Gober for the extensive use of his fluorescence microscope; P. Marc for constructing the pUG35-Rnt1p plasmid and help with early studies; J. Aris, M. Caizergues-Ferrer, Y. Henry, T. Meier, and M. Nomura for yeast strains and/or antibodies; P.E. Gleyzes for providing the pre-rRNA FISH protocol and the rRNA oligonucleotide probe; S. Baserga, J. Gallagher, M. Grunstein, and D. Robyr for chromatin immunoprecipitation protocols; and D. Black and H. Martinson for critical reading of the manuscript. This work was supported by a long-term EMBO Postdoctoral Fellowship and by a Human Frontier Long-Term Postdoctoral Fellowship (A.H.) and by grant GM61518 from National Institutes of Health (NIH) to G.C.

The publication costs of this article were defrayed in part by payment of page charges. This article must therefore be hereby marked "advertisement" in accordance with 18 USC section 1734 solely to indicate this fact.

Received April 29, 2004; accepted July 15, 2004.

REFERENCES

Abou Elela, S. and Ares Jr., M. 1998. Depletion of yeast RNase III blocks correct U2 3′ end formation and results in polyadenylated but functional U2 snRNA. *EMBO J.* **17:** 3738–3746.

Abou Elela, S., Igel, H., and Ares Jr., M. 1996. RNase III cleaves eukaryotic preribosomal RNA at a U3 snoRNP-dependent site. *Cell* **85:** 115–124.

Allmang, C. and Tollervey, D. 1998. The role of the 3′ external transcribed spacer in yeast pre-rRNA processing. *J. Mol. Biol.* **278:** 67–78.

Allmang, C., Kufel, J., Chanfreau, G., Mitchell, P., Petfalski, E., and Tollervey, D. 1999. Functions of the exosome in rRNA, snoRNA and snRNA synthesis. *EMBO J.* **18:** 5399–5410.

Baudin, A., Ozier-Kalogeropoulos, O., Denouel, A., Lacroute, F., and Cullin, C. 1993. A simple and efficient method for direct gene deletion in *Saccharomyces cerevisiae*. *Nucleic Acids Res.* **21:** 3329–3330.

Catala, M., Lamontagne, B., Larose, S., Ghazal, G., and Abou Elela, S. 2004. Cell cycle dependent nuclear localization of yeast RNase III is required for efficient cell division. *Mol. Biol. Cell.* **15:** 3015–3030.

Chanfreau, G., Elela, S.A., Ares Jr., M., and Guthrie, C. 1997. Alternative 3′-end processing of U5 snRNA by RNase III. *Genes & Dev.* **11:** 2741–2751.

Chanfreau, G., Legrain, P., and Jacquier, A. 1998a. Yeast RNase III as a key processing enzyme in small nucleolar RNAs metabolism. *J. Mol. Biol.* **284:** 975–988.

Chanfreau, G., Rotondo, G., Legrain, P., and Jacquier, A. 1998b. Processing of a dicistronic small nucleolar RNA precursor by the RNA endonuclease Rnt1. *EMBO J.* **17:** 3726–3737.

Chanfreau, G., Buckle, M., and Jacquier, A. 2000. Recognition of a conserved class of RNA tetraloops by *Saccharomyces cerevisiae* RNase III. *Proc. Natl. Acad. Sci.* **97:** 3142–3147.

Cuadros-Fernandez, J.M. and Esponda, P. 1996. Immunocytochemical localisation of the nucleolar protein fibrillarin and RNA polymerase I during mouse early embryogenesis. *Zygote* **4:** 49–58.

Danin-Kreiselman, M., Lee, C.Y., and Chanfreau, G. 2003. RNAse III-mediated degradation of unspliced pre-mRNAs and lariat introns. *Mol. Cell* **11:** 1279–1289.

Dingwall, C. and Laskey, R.A. 1991. Nuclear targeting sequences—A consensus? *Trends Biochem. Sci.* **16:** 478–481.

Fath, S., Milkereit, P., Podtelejnikov, A.V., Bischler, N., Schultz, P., Bier, M., Mann, M., and Tschochner, H. 2000. Association of yeast RNA polymerase I with a nucleolar substructure active in rRNA synthesis and processing. *J. Cell Biol.* **149:** 575–590.

Garcia-Blanco, M.A., Miller, D.D., and Sheetz, M.P. 1995. Nuclear spreads: I. Visualization of bipartite ribosomal RNA domains. *J. Cell Biol.* **128:** 15–27.

Ho, Y., Gruhler, A., Heilbut, A., Bader, G.D., Moore, L., Adams, S.L., Millar, A., Taylor, P., Bennett, K., Boutilier, K., et al. 2002. Systematic identification of protein complexes in *Saccharomyces cerevisiae* by mass spectrometry. *Nature* **415:** 180–183.

Hozak, P., Jackson, D.A., and Cook, P.R. 1994. Replication factories and nuclear bodies: The ultrastructural characterization of replication sites during the cell cycle. *J. Cell Sci.* **107:** 2191–2202.

Huh, W.K., Falvo, J.V., Gerke, L.C., Carroll, A.S., Howson, R.W., Weissman, J.S., and O'Shea, E.K. 2003. Global analysis of protein localization in budding yeast. *Nature* **425:** 686–691.

Ito, T., Chiba, T., Ozawa, R., Yoshida, M., Hattori, M., and Sakaki, Y. 2001. A comprehensive two-hybrid analysis to explore the yeast protein interactome. *Proc. Natl. Acad. Sci.* **98:** 4569–4574.

Jackson, D.A. and Cook, P.R. 1995. The structural basis of nuclear function. *Int. Rev. Cytol.* **162A:** 125–149.

Kufel, J., Dichtl, B., and Tollervey, D. 1999. Yeast Rnt1p is required for cleavage of the pre-ribosomal RNA in the 3′ ETS but not the 5′ ETS. *RNA* **5:** 909–917.

Lamontagne, B., Tremblay, A., and Abou Elela, S. 2000. The N-terminal domain that distinguishes yeast from bacterial RNase III contains a dimerization signal required for efficient double-stranded RNA cleavage. *Mol. Cell. Biol.* **20:** 1104–1115.

Lamontagne, B., Larose, S., Boulanger, J., and Elela, S.A. 2001. The RNase III family: A conserved structure and expanding functions in eukaryotic dsRNA metabolism. *Curr. Issues Mol. Biol.* **3:** 71–78.

Lazdins, I.B., Delannoy, M., and Sollner-Webb, B. 1997. Analysis of nucleolar transcription and processing domains and pre-rRNA movements by in situ hybridization. *Chromosoma* **105:** 481–495.

Lee, C.Y., Lee, A., and Chanfreau, G. 2003. The roles of endonucleolytic cleavage and exonucleolytic digestion in the 5′-end processing

of *S. cerevisiae* box C/D snoRNAs. *RNA* **9:** 1362–1370.
Leger-Silvestre, I., Trumtel, S., Noaillac-Depeyre, J., and Gas, N. 1999. Functional compartmentalization of the nucleus in the budding yeast *Saccharomyces cerevisiae*. *Chromosoma* **108:** 103–113.
Liljelund, P., Mariotte, S., Buhler, J.M., and Sentenac, A. 1992. Characterization and mutagenesis of the gene encoding the A49 subunit of RNA polymerase A in *Saccharomyces cerevisiae*. *Proc. Natl. Acad. Sci.* **89:** 9302–9305.
Mosgoeller, W., Schofer, C., Wesierska-Gadek, J., Steiner, M., Muller, M., and Wachtler, F. 1998. Ribosomal gene transcription is organized in foci within nucleolar components. *Histochem. Cell. Biol.* **109:** 111–118.
Nagel, R. and Ares Jr., M. 2000. Substrate recognition by a eukaryotic RNase III: The double-stranded RNA-binding domain of Rnt1p selectively binds RNA containing a 5′-AGNN-3′ tetraloop. *RNA* **6:** 1142–1156.
Nicholson, A.W. 1999. Function, mechanism and regulation of bacterial ribonucleases. *FEMS Microbiol. Rev.* **23:** 371–390.
Niedenthal, R.K., Riles, L., Johnston, M., and Hegemann, J.H. 1996. Green fluorescent protein as a marker for gene expression and subcellular localization in budding yeast. *Yeast* **12:** 773–786.
Oakes, M., Aris, J.P., Brockenbrough, J.S., Wai, H., Vu, L., and Nomura, M. 1998. Mutational analysis of the structure and localization of the nucleolus in the yeast *Saccharomyces cerevisiae*. *J. Cell Biol.* **143:** 23–34.
Prescott, E.M., Osheim, Y.N., Jones, H.S., Alen, C.M., Roan, J.G., Reeder, R.H., Beyer, A.L., and Proudfoot, N.J. 2004. Transcriptional termination by RNA polymerase I requires the small subunit Rpa12p. *Proc. Natl. Acad. Sci.* **101:** 6068–6073.
Qu, L.H., Henras, A., Lu, Y.J., Zhou, H., Zhou, W.X., Zhu, Y.Q., Zhao, J., Henry, Y., Caizergues-Ferrer, M., and Bachellerie, J.P. 1999. Seven novel methylation guide small nucleolar RNAs are processed from a common polycistronic transcript by Rat1p and RNase III in yeast. *Mol. Cell. Biol.* **19:** 1144–1158.
Reeder, R.H., Guevara, P., and Roan, J.G. 1999. *Saccharomyces cerevisiae* RNA polymerase I terminates transcription at the Reb1 terminator in vivo. *Mol. Cell. Biol.* **19:** 7369–7376.
Seipelt, R.L., Zheng, B., Asuru, A., and Rymond, B.C. 1999. U1 snRNA is cleaved by RNase III and processed through an Sm site-dependent pathway. *Nucleic Acids Res.* **27:** 587–595.
Storici, F., Lewis, L.K., and Resnick, M.A. 2001. In vivo site-directed mutagenesis using oligonucleotides. *Nat. Biotechnol.* **19:** 773–776.
Thompson, M., Haeusler, R.A., Good, P.D., and Engelke, D.R. 2003. Nucleolar clustering of dispersed tRNA genes. *Science* **302:** 1399–1401.
Tremblay, A., Lamontagne, B., Catala, M., Yam, Y., Larose, S., Good, L., and Elela, S.A. 2002. A physical interaction between Gar1p and Rnt1p is required for the nuclear import of H/ACA small nucleolar RNA-associated proteins. *Mol. Cell. Biol.* **22:** 4792–4802.
Trumtel, S., Leger-Silvestre, I., Gleizes, P.E., Teulieres, F., and Gas, N. 2000. Assembly and functional organization of the nucleolus: Ultrastructural analysis of *Saccharomyces cerevisiae* mutants. *Mol. Biol. Cell* **11:** 2175–2189.
Verheggen, C., Mouaikel, J., Thiry, M., Blanchard, J.M., Tollervey, D., Bordonne, R., Lafontaine, D.L., and Bertrand, E. 2001. Box C/D small nucleolar RNA trafficking involves small nucleolar RNP proteins, nucleolar factors and a novel nuclear domain. *EMBO J.* **20:** 5480–5490.
Warner, J.R. 1999. The economics of ribosome biosynthesis in yeast. *Trends Biochem. Sci.* **24:** 437–440.
Wu, H., Henras, A., Chanfreau, G., and Feigon, J. 2004. Structural basis for recognition of the AGNN tetraloop RNA fold by the double-stranded RNA-binding domain of Rnt1p RNase III. *Proc. Natl. Acad. Sci.* **101:** 8307–8312.

A cotranscriptional model for 3′-end processing of the *Saccharomyces cerevisiae* pre-ribosomal RNA precursor

ANTHONY K. HENRAS, EDOUARD BERTRAND and GUILLAUME CHANFREAU

RNA 2004 10: 1572-1585